Organic & Biomolecular Chemistry

RSC Publishing

PAPER

View Article Online
View Journal

Photoresponsive two-component organogelators based on trisphenylisoxazolylbenzene†

Cite this: DOI: 10.1039/c3ob00041a

Takeharu Haino,* Yuko Hirai, Toshiaki Ikeda and Hiroshi Saito

Received 9th January 2013,
Accepted 10th April 2013

DOI: 10.1039/c3ob00041a

www.rsc.org/obc

Photochromic tris(phenylisoxazolyl)benzene **1** and bispyridine derivatives **2a–e** were mixed in a certain ratio to generate stable gels in benzyl alcohol, 4-methoxybenzyl alcohol, and aniline. Supramolecular assembly of **1** in solution was confirmed by ^{1}H NMR study. The T_{gel} value was saturated in a 2 : 3 ratio of **1** and **2c**. The intermolecular hydrogen bonds OH···N and salt bridge O$^-$···H–N$^+$ between **1** and **2c** coexisted evidently, and these hydrogen bonds contributed to the stabilization of the gel networks. The lengths of alkyl chains of **2a–e** governed the stabilities of the gels. The gel formations were driven by the morphological transition of **1** before and after the addition of **2a–e**. Mixtures of **1** and **2a–e** led to the well developed fibrillar networks, generating a lot of voids that are responsible for immobilizing solvent molecules. When the benzyl alcohol gel was irradiated at 360 nm, the gel turned to the sol. The sol was reversed to the gel by warming. This gel-to-sol phase transition was completely reversible.

Introduction

Molecular organogels of low-molecular-weight organogelators (LMOGs) are thermally reversible viscoelastic materials, formed by self-assembly *via* noncovalent interactions.[1] The aggregation of gelators forms the entangled fibers, giving rise to the three-dimensional network.[2] Solvent molecules are immobilized in voids of the network, which are responsible for gelation. The properties of LMOGs rely on the nature of their resulting three-dimensional supramolecular organizations in which the molecular constituents are spatially organized.[3] Control of these organization processes by chemical or physical stimuli represents a prime scientific challenge to develop stimuli-responsive functional materials.[4] Integration of photochromic units as an addressable functionality onto the molecular constituents offers potential access to achieve the reversible control of the organization process that induces a sol-to-gel transition.[5] Therefore, LMOGs possessing photochromic units have become a groundbreaking area in the field of material chemistry. The development of a desired photochromic LMOG requires a lot of synthetic efforts to provide structural variants, because a tiny structural modification of a gelator can appreciably influence its gelation ability. Two-component LMOGs[6] functionalized with a photochromic moiety are synthetically more accessible than a conventional LMOG—the photochromic unit and a long alkyl side chain are separately placed in each of the components that are connected through noncovalent interaction.[7]

We have previously reported that an isoxazolyl ring is a key functionality for generating molecular assemblies,[8] *e.g.* tris(phenylisoxazolyl)benzenes assembled to form fibrillar gel networks in common organic solvents,[9] and an azobenzene functionalized gelator[10] showed a photoresponsive nature. Here, we report a new class of two-component photochromic LMOGs composed of photochromic tris(phenylisoxazolyl)benzene **1**[10] and bispyridines **2a–e** (Scheme 1). **1** has three phenolic hydroxyl groups that are responsible for hydrogen bonding interactions. Long alkyl chains are introduced onto the bispyridine unit. When **1** and **2a–e** are blended in a certain ratio, the fibrous assemblies of **1** should be cross-linked by **2a–e**, forming hydrogen bonds between the phenolic hydroxyl group and the pyridine nitrogen.

Result and discussion

Self-assembling behavior

The self-assembling behavior of **1** was examined in DMSO-d_6 using ^{1}H NMR spectroscopy. Aromatic protons H_a–H_f appeared in a common aromatic region at concentrations lower than 1 mmol L^{-1} (Fig. 1). Upon concentrating the solution of **1**, every aromatic resonance shifted upfield, suggesting that **1** assembled as piles in which each aromatic proton experiences the shielding effect of the neighboring aromatic groups.

Department of Chemistry, Graduate School of Science, Hiroshima University, 1-3-1 Kagamiyama, Higashi-Hiroshima, 739-8526, Japan.
E-mail: haino@hiroshima-u.ac.jp; Fax: +81-82-424-0724; Tel: +81-82-424-7427

†Electronic supplementary information (ESI) available: Analysis of self-association by ^{1}H NMR experiments, gelation properties, UV/vis absorption spectra, AFM images, and ^{1}H and ^{13}C NMR spectra of all new compounds. See DOI: 10.1039/c3ob00041a

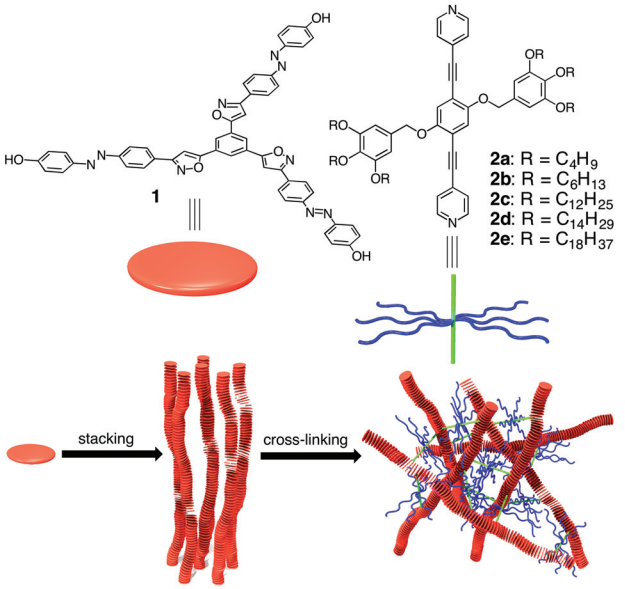

Scheme 1 Photochromic tris(phenylisoxazolyl)benzene **1** and bispyridines **2a–e**, and the schematic representation of gel formation.

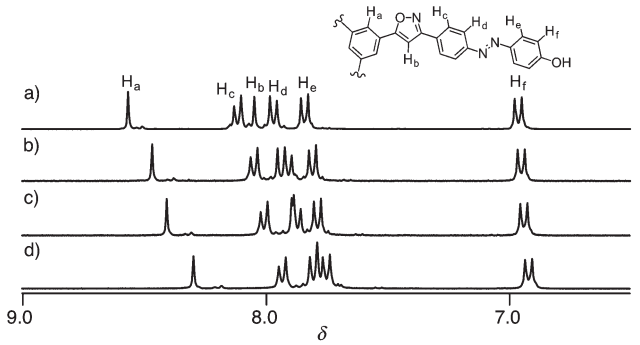

Fig. 1 ^{1}H NMR spectra of **1** at concentrations of (a) 1.0, (b) 3.0, (c) 5.0, and (d) 10.0 mmol L^{-1} in DMSO-d_6.

Plotting the chemical shift changes of the protons *versus* the concentration of **1** produced hyperbolic curves. By applying the isodesmic model (see the ESI†), nonlinear regression analysis of the curves gave rise to the estimated complexation-induced shifts ($\Delta\delta$ = −1.04, −1.01, −0.70, −0.60, −0.36, and −0.17 ppm for H_a, H_b, H_c, H_d, H_e, and H_f) and the association constant of 87 ± 5 L mol^{-1}. The complexation-induced shifts decreased with increasing distance of the protons from the C_3 axis of **1**, implying that **1** stacked as piles along the C_3 axis. This can lead to the formation of polymeric fibrillar assemblies.

Gelation properties

The gelation tests of **1**, **2a–e**, and their mixtures were performed using the "invert test-tube" method. The compounds and solvents were placed in a screw-capped test tube and warmed until the solids dissolved. The solution was then cooled to 298 K and left for 2 h under ambient conditions. The

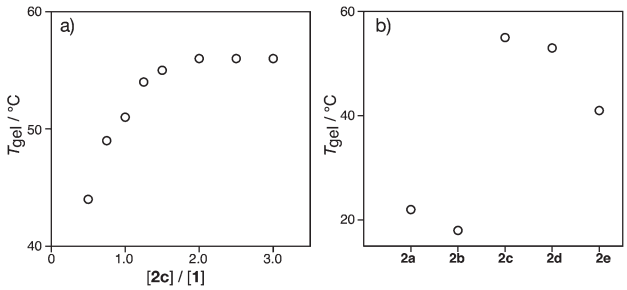

Fig. 2 Gelation temperatures (T_{gel}) of solutions of **1** (3 g L^{-1}) in *p*-methoxybenzyl alcohol (a) in the presence of **2c**, and (b) in the presence of **2a–e** in a ratio of 2 : 3 for **1** and **2a–e**.

gelation was confirmed by the absence of the gravitational flow of solvents when the test tube was inverted. The gelation properties of **1**, **2a–e**, and their mixtures were examined in twenty-nine solvents (Table S1†). **1** and **2a–e** were not gelators. The mixtures of **1** and **2a–e** formed gels in benzyl alcohol, in aniline, and in *p*-methoxybenzyl alcohol.

To discuss the gel stability upon mixing **1** and **2c**, the sol–gel phase transitions were examined by measuring the gel melting temperature (T_{gel}) in *p*-methoxybenzyl alcohol and benzyl alcohol (Fig. 2a and S1†). The solution of **1** ([**1**] = 3 g L^{-1}) became viscous upon the addition of **2c**, and T_{gel} values were determined. The gelation was appreciably influenced by ratios of **1** and **2c**. With increasing the concentration of **2c**, the gel became stable. The highest T_{gel} value was obtained in a 2 : 3 ratio of **1** and **2c**. Further addition of **2c** did not influence the gel stability. These values provide quite a reasonable agreement with the ratio of the numbers of the acidic phenol units to the basic pyridyl units, implying that hydrogen bonds between the phenolic hydroxyl and the pyridyl moieties most likely contribute to the stabilization of the gel networks.

To confirm the formation of the hydrogen bonding between the phenolic hydroxyl and the basic nitrogen of pyridyl ring, titration experiments were carried out in THF. **1** has a strong UV-vis absorption band at 367 nm, which are sensitive to hydrogen bonding interaction with the hydroxyl groups.[11] Bispyridine **2c** has a UV-vis absorption band at approximately 370 nm, which was completely overlapped with that of **1**. Then, 4-dimethylaminopyridine (DMAP) was employed for the titration of **1** instead of **2c**. Upon the addition of DMAP, the absorption maximum of **1** red-shifted from 367 nm to 374 nm with isosbestic point, indicating the formation of the intermolecular OH···N hydrogen bond (Fig. S2a†). This spectral characteristic was highly influenced by solvent properties; in benzyl alcohol, the absorption band at 371 nm decreased while the new band at 475 nm emerged upon the addition of DMAP (Fig. S2b†). The same characteristics of the spectral shifts were observed when sodium hydroxide was added instead of DMAP (Fig. S2c†). The traits support that the phenolic protons of the azobenzene units were partially removed by DMAP; as a result, the intermolecular OH···N hydrogen bond and the salt bridge $O^-\cdots H\text{–}N^+$ coexisted.

The gelation properties are also governed by the dimensions of the alkyl chains of **2a–e**. With increasing the length of the side chains, the gels were thermally stabilized (Fig. 2b). The gel stabilities were maximized in the presence of **2c,d**, whereas **2e** reduced the stability. **2e** showed lower solubility to the solvents than **2c,d**; thereby, the highly lipophilic nature of **2e** resulted in its quick precipitation before the gel formed.

Morphologies

To obtain a detailed insight into the two-component gel system, morphologies of the films prepared by casting solutions of **1**, **2a–e**, and mixtures of **1** and **2a–e** were investigated by scanning electron microscopy (SEM). Fig. 3a and b showed microcrystalline and tape-like morphologies, which most probably resulted from the self-assembly of **1**. Morphologies of films of **2a–e** were altered by the dimensions of the alkyl side chains. *n*-Butyl and *n*-hexyl side chains were probably too short to form well-developed three-dimensional nanostructures (Fig. 3c–f). By contrast, flower-like morphologies were found in the film, prepared from a benzyl alcohol solution of **2c**. Aniline solvent facilitated the anisotropic growth of **2c** that resulted in the helical tape-like nanostructures (Fig. 3h). *n*-Tetradecyl side chains of **2d** stabilized the helical tape-like nanostructures, the entanglement of which generated the well developed three dimensional networks (Fig. 3i,j). **2e** mostly produced the film-like morphologies in both solvents (Fig. 3k,l). The fibrillar morphologies were partially found, and bundled into film-like morphologies. The stability of the helical tape-like nanostructures was apparently determined by the dimensions of the aliphatic side chains. The self-assembly of **2c,d** is most probably driven by the phase separation of the aliphatic and the aromatic moieties. The rigid aromatic cores can be capable of assembling with the assistance of aromatic stacking interaction, and the assemblies are thereby surrounded by long alkyl chains. The helical tape-like nanostructures perhaps result from further aggregation of the rod-like supramolecular structures in the solid state.

Upon mixing azobenzene **1** and bispyridines **2a–e** in a ratio of 2 : 3 in benzyl alcohol and in aniline, the xerogels resulted in dramatic morphological changes. The helical, flower-like, and tape-like morphologies turned into highly developed and entangled fibrillar networks that were confirmed by the SEM images (Fig. 4a–j). The anisotropic growth of the assemblies of mixtures of **1** and **2a–e** generated the long and entangled gel fibers that gave rise to a lot of voids. Especially, a mixture of **1** and **2d** or **2e** gave rise to well-developed three-dimensional networks.

Employing atomic force microscopy measurements of cast films of **1** with or without **2c** gained an insight into the supramolecular assemblies of **1** and **2c**. The assembly of **1** gave rise to the well developed fibers that bundled with an average cross-section of 1.5 ± 0.1 nm (Fig. 5a, S3†), whereas cast-films from solutions of **2c** provided only amorphous morphologies (Fig. S4†). By contrast, the presence of bispyridyl linker **2c** led **1** to thicker sheet-like morphologies in which fibers could directionally align to form bundles (Fig. 5b, S5†). The cross-sections increased to be more than 2.5 nm in THF. Benzyl alcohol and aniline solvents produced further growth of the fibers, the cross-section of which reached more than 3.0 nm (Fig. S6†). Fig. 5c,d indicates that the interconnection of the fibrillar assemblies promoted bundling of them to form thicker supramolecular networks, which should be facilitated by the bispyridyl linkages.

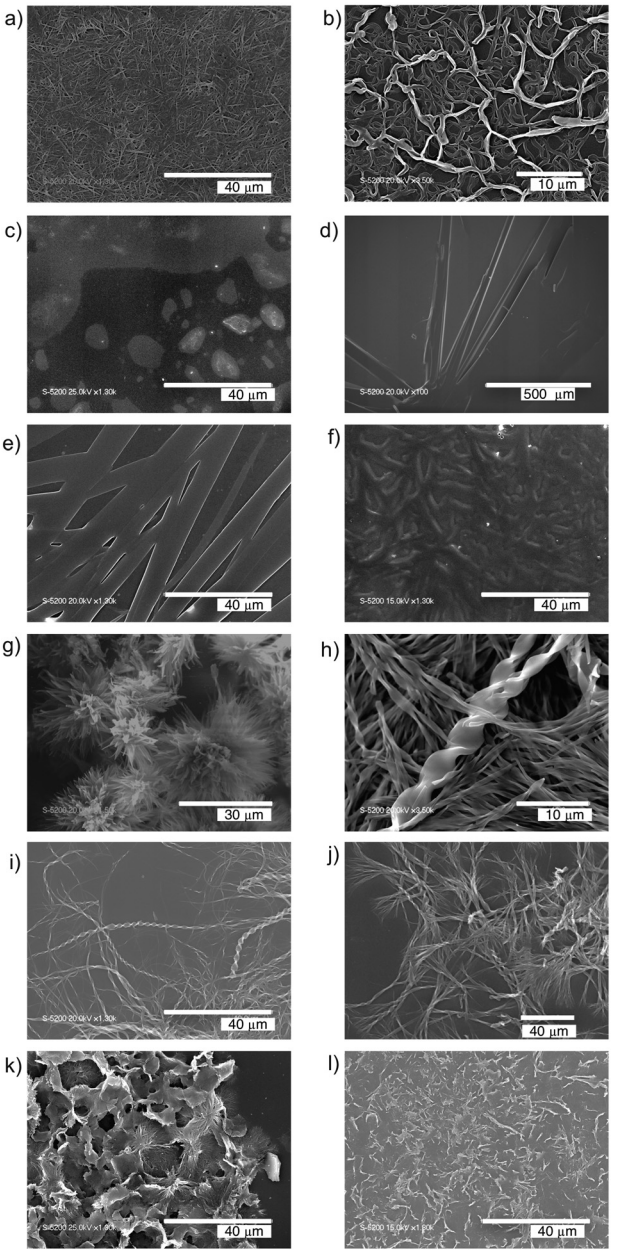

Fig. 3 SEM images of cast-films of (a, b) **1**, (c, d) **2a**, (e, f) **2b**, (g, h) **2c**, (i, j) **2d**, and (k, l) **2e** in (a, c, e, g, i, k) benzyl alcohol and (b, d, f, h, j, l) aniline.

Photoisomerization

Photoisomerization of *trans*-isomer of **1** was monitored by UV-vis absorption spectroscopy (Fig. 6). A solution of *trans*-isomer

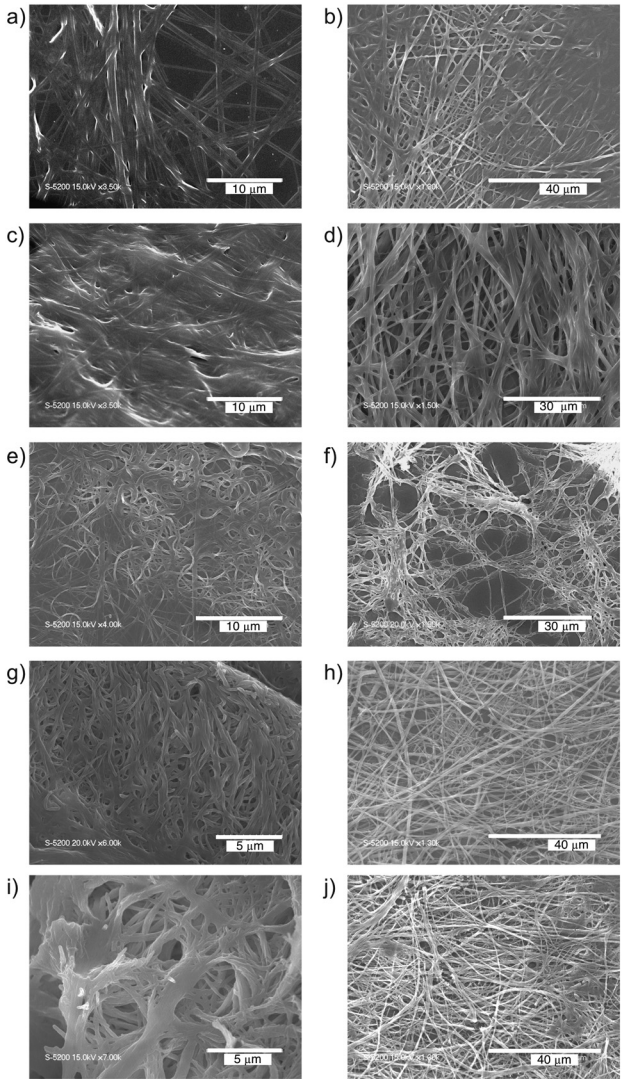

Fig. 4 SEM images of cast-films of **1** in the presence of (a, b) **2a**, (c, d) **2b**, (e, f) **2c**, (g, h) **2d**, and (i, j) **2e** in (a, c, e, g, i) benzyl alcohol and (b, d, f, h, j) aniline.

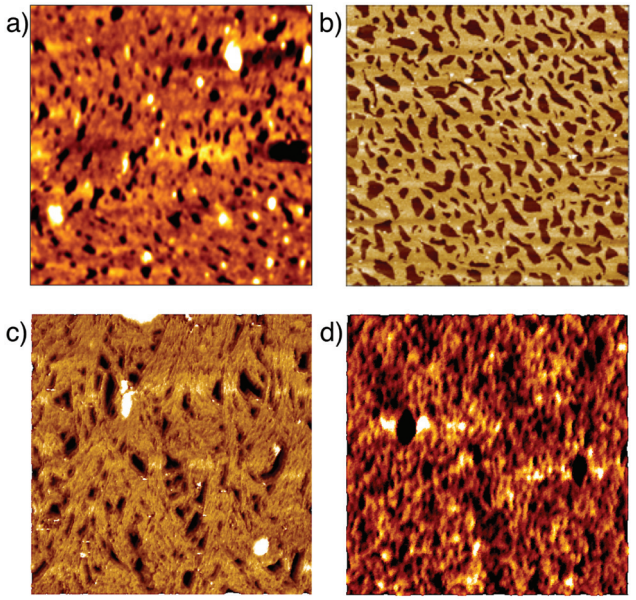

Fig. 5 AFM images of cast-films on mica prepared from solutions of (a) **1** in THF (1 μm × 1 μm) and **1** with **2c** (b) in THF (5 μm × 5 μm), (c) in benzyl alcohol (2.5 μm × 2.5 μm), and (d) in aniline (1 μm × 1 μm).

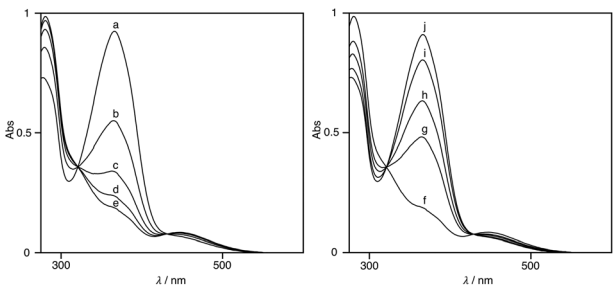

Fig. 6 Absorption spectra of *trans*-isomer of **1** (8.4×10^{-6} mol L^{-1}) in THF: (left) the process of *trans–cis* isomerization under irradiation with 360 nm light; (right) the subsequent reverse isomerization process under irradiation with 450 nm light. (a–e) 0, 5, 10, 15, 20 min; (f–j) 0, 5, 10, 30, 60 min.

Fig. 7 The gel-to-sol transition of a mixture of **1** and **2c** in benzyl alcohol at room temperature. The pictures are: (left) before UV irradiation, (middle) after UV irradiation, and (right) after warming.

in THF showed a sharp absorption band at approximately 360 nm and a broad band around 450 nm, assigned as the π–π* and n–π* transitions of the azobenzene moieties. Upon irradiation at 360 nm, the band at 360 nm decreased and a new broad band simultaneously emerged at 445 nm. These changes produced the isosbestic points at 320 and 431 nm, indicating that the photoisomerization was a unimolecular process in which only two chemical species existed. Accordingly, the *trans*-isomer was converted to the *cis*-isomer as a primary product. The *cis*-isomer turned back to the *trans*-isomer by irradiation of 460 nm light. These processes showed complete reversibility.

In our previous study, the *cis*-isomer is not capable of generating stacked supramolecular assemblies.[10] Therefore, the sol-to-gel transition can be switchable in the two component organogelators through the photo-induced structural isomerization. The turbid gel prepared from a solution of **1** and **2c** in benzyl alcohol was stable when the tube was turned upside down (Fig. 7, left). Under the irradiation of UV light at 365 nm for several hours, the gel became transparent sol (Fig. 7, middle), indicating that the *trans*-isomer isomerized to the *cis*-isomer, collapsing the stable gel. Once the resulting sol was warmed up, the *cis*-to-*trans* thermal isomerization was promoted, and the *trans*-isomers gave rise to the turbid gel (Fig. 7,

right). The effective self-assembling of the *trans*-isomer is most likely responsible for the gel formation, whereas the reasonably weaker molecular interaction of the *cis*-isomer destroys the higher order of supramolecular assemblies even though they are connected by the bispyridyl linker *via* hydrogen bonds.

Conclusions

Photoresponsive organogelators were synthetically accessible through the two-component system composed of tris(phenylisoxazolyl)benzene **1** and bispyridines **2a–e** acting as a supramolecular linker that connected the fibrillar assemblies of **1**. The gel-to-sol phase changes were successfully controlled through the photo-induced structural isomerization of the azobenzene moieties. These results propose a way of exploiting new photoresponsive low-molecular-weight organogelators.

Experimental

General

All chemicals were used without further purification unless otherwise specified. Flash column chromatography was performed employing 200–300 mesh silica gel. Proton and carbon NMR spectra were recorded on a Varian Mercury-300 spectrometer. IR spectra were obtained on a JASCO FT/IR-420S. UV-vis absorption spectra were measured on a JASCO V-560 spectrometer. Mass spectra were reported with a Thermo Fisher Scientific LTQ Orbitrap XL. Melting points were measured with an AS ONE micro melting point apparatus and uncorrected. Elemental analyses were performed on a Perkin-Elmer 2400CHN elemental analyser. Atomic Force Microscopy measurements were carried out by using an Agilent 5100 AFM system. SEM images were obtained by Hitachi S-5200 field emission scanning electron microscopy.

1,4-Diiodo-2,5-bis{[3,4,5-tri(butoxy)phenyl]methoxy}benzene (3). 2,5-Diiodohydroquinone (517 mg, 1.43 mmol), 3,4,5-tri(butoxy)benzyl chloride (1.22 g, 3.56 mmol), potassium carbonate (1.2 g, 8.56 mmol), and 15 mL DMF were mixed in a round bottom flask, and the mixture was stirred at 50 °C for 24 h under an argon atmosphere. The reaction mixture was cooled to room temperature, and poured into 250 mL of ice-cold water. The aqueous layer was extracted with ethyl acetate twice. The combined organic layer was washed with brine (50 mL), dried over anhydrous sodium sulfate, and concentrated. The crude product was purified by column chromatography on silica gel (5% ethyl acetate–hexane) to obtain the pure product as a white powder (995 mg, 71%). M.p. 84–85 °C; ^{1}H NMR (300 MHz, chloroform-d$_1$) δ 7.27 (s, 2H), 6.69 (s, 4H), 4.97 (s, 4H), 4.01 (t, 8H, J = 6.5 Hz), 3.97 (t, 4H, J = 6.5 Hz), 1.67–1.85 (m, 12H), 1.43–1.60 (m, 12H), 0.97 (t, 12H, J = 7.4 Hz), and 0.96 (t, 6H, J = 7.4 Hz) ppm; ^{13}C NMR (75 MHz, chloroform-d$_1$) δ 153.2, 152.7, 137.8, 131.1, 123.7, 105.7, 86.6, 73.0, 72.2, 68.8, 32.3, 31.4, 19.3, 19.2, 13.9, and 13.9 ppm; HRMS (ESI$^+$) calcd for $C_{44}H_{64}O_8I_2Na$ m/z 997.2583 [M + Na]$^+$, found m/z 997.2582; Anal. calcd for $C_{44}H_{64}O_8I_2$ C 54.21, H 6.62, found C 54.32, H 6.52%.

1,4-Diiodo-2,5-bis{[3,4,5-tri(hexoxy)phenyl]methoxy}benzene (4). 2,5-Diiodohydroquinone (543 mg, 1.50 mmol), 3,4,5-tri(hexoxy)benzyl chloride (1.41 g, 3.30 mmol), potassium carbonate (1.3 g, 9.0 mmol), and 15 mL DMF were mixed in a round bottom flask, and the mixture was stirred at 50 °C for 24 h under an argon atmosphere. The reaction mixture was cooled to room temperature, and poured into 250 mL of ice-cold water. The aqueous layer was extracted with chloroform twice. The combined organic layer was washed with brine (50 mL), dried over anhydrous sodium sulfate, and concentrated. The crude product was purified by column chromatography on silica gel (5% ethyl acetate–hexane) to obtain the pure product as a white powder (1.57 g, 91%). M.p. 71–74 °C; ^{1}H NMR (300 MHz, chloroform-d$_1$) δ 7.27 (s, 2H), 6.69 (s, 4H), 4.97 (s, 4H), 4.00 (t, 8H, J = 6.5 Hz), 3.95 (t, 4H, J = 6.5 Hz), 1.69–1.86 (m, 12H), 1.41–1.58 (m, 12H), 1.24–1.39 (m, 24H), and 0.85–0.95 (m, 18H) ppm; ^{13}C NMR (75 MHz, chloroform-d$_1$) δ 153.2, 152.7, 137.7, 131.1, 123.6, 105.6, 86.6, 73.4, 72.1, 69.1, 31.7, 31.5, 30.2, 29.3, 25.8, 22.7, 22.6, 14.1, and 14.0 ppm; HRMS (ESI$^+$) calcd for $C_{56}H_{88}O_8I_2Na$ m/z 1165.4461 [M + Na]$^+$, found m/z 1165.4464; Anal. calcd for $C_{56}H_{88}O_8I_2$ C 58.84, H 7.76, found C 59.11, H 7.74%.

1,4-Diiodo-2,5-bis{[3,4,5-tri(tetradecoxy)phenyl]methoxy}-benzene (5). 2,5-Diiodohydroquinone (108 mg, 0.297 mmol), 3,4,5-tri(tetradecoxy)benzyl chloride (500 mg, 0.654 mmol), potassium carbonate (0.31 g, 1.7 mmol), and 3 mL DMF were mixed in a round bottom flask, and the mixture was stirred at 50 °C for 24 h under an argon atmosphere. The reaction mixture was cooled to room temperature, and poured into 250 mL of ice-cold water. The aqueous layer was extracted with chloroform twice. The combined organic layer was washed with brine (50 mL), dried over anhydrous sodium sulfate, and concentrated. The crude product was purified by column chromatography on silica gel (5% ethyl acetate–hexane) to obtain the pure product as a white powder (362 mg, 69%). M.p. 57–60 °C; ^{1}H NMR (300 MHz, chloroform-d$_1$) δ 7.27 (s, 2H), 6.69 (s, 4H), 4.96 (s, 4H), 3.99 (t, 8H, J = 6.5 Hz), 3.95 (t, 4H, J = 6.5 Hz), 1.69–1.86 (m, 12H), 1.41–1.58 (m, 12H), 1.24–1.39 (m, 120H), and 0.85–0.95 (m, 18H) ppm; ^{13}C NMR (75 MHz, chloroform-d$_1$) δ 153.2, 152.7, 137.8, 131.1, 123.6, 105.6, 86.6, 73.4, 72.1, 69.1, 31.9, 31.9, 30.3, 29.8, 29.7, 29.7, 29.6, 29.4, 29.4, 26.1, 22.7, and 14.1 ppm; HRMS (ESI$^+$) calcd for $C_{104}H_{184}O_8I_2Na$ m/z 1838.1923 [M + Na]$^+$, found m/z 1838.1974; Anal. calcd for $C_{104}H_{184}O_8I_2$ C 68.77, H 10.21, found C 69.11, H 9.92%.

1,4-Diiodo-2,5-bis{[3,4,5-tri(octadecoxy)phenyl]methoxy}-benzene (6). 2,5-Diiodohydroquinone (254 mg, 0.701 mmol), 3,4,5-tri(octadecoxy)benzyl chloride (1.63 g, 1.75 mmol), potassium carbonate (0.50 g, 4.2 mmol), and 3 mL DMF were mixed in a round bottom flask, and the mixture was stirred at 50 °C for 24 h under an argon atmosphere. The reaction mixture was cooled to room temperature, and poured into 250 mL of ice-cold water. The aqueous layer was extracted with

chloroform twice. The combined organic layer was washed with brine (50 mL), dried over anhydrous sodium sulfate, and concentrated. The crude product was purified by column chromatography on silica gel (5% ethyl acetate–hexane) to obtain the pure product as a white powder (1.24 g, 82%). M.p. 70–73 °C; ^{1}H NMR (300 MHz, chloroform-d_1) δ 7.27 (s, 2H), 6.69 (s, 4H), 4.96 (s, 4H), 3.99 (t, 8H, J = 6.5 Hz), 3.95 (t, 4H, J = 6.5 Hz), 1.69–1.86 (m, 12H), 1.41–1.58 (m, 12H), 1.24–1.39 (m, 168H), and 0.85–0.95 (m, 18H) ppm; ^{13}C NMR (75 MHz, chloroform-d_1) δ 153.2, 152.7, 137.8, 131.1, 123.6, 105.6, 86.6, 73.4, 72.2, 69.1, 31.9, 30.3, 29.7, 29.7, 29.5, 29.4, 26.1, 22.7, and 14.1 ppm; HRMS (ESI$^+$) calcd for $C_{128}H_{232}O_8I_2Na$ m/z 2174.5729 $[M + Na]^+$, found m/z 2174.5732; Anal. calcd for $C_{56}H_{88}O_8I_2$ C 71.41, H 10.86, found C 71.36, H 10.93%.

1,4-Bis(4′-pyridylethynyl)-2,5-bis{[3,4,5-tri(butoxy)phenyl]-methoxy}benzene (2a). A mixture of **4** (550 mg, 0.564 mmol), 4-ethynylpyridine (175 mg, 1.69 mmol), $PdCl_2(PPh_3)_2$ (20.1 mg, 28 μmol), and CuI (5.3 mg, 28 μmol) in dry THF (6 mL) and dry diisopropylamine (1.6 mL) was stirred for 6 h at rt. The reaction mixture was diluted with ethyl acetate, and the resulting insoluble solid was filtered off. The organic layer was washed with aqueous ammonium chloride solution, dried over anhydrous sodium sulfate, and concentrated. The crude product was purified through recrystallization from ethyl acetate to give a yellow powder (480 mg, 53%). M.p. 165–167 °C; ^{1}H NMR (300 MHz, chloroform-d_1) δ 8.59 (d, 4H, J = 5.9 Hz), 7.34 (d, 4H, J = 5.9 Hz), 7.13 (s, 2H), 6.69 (s, 4H), 5.06 (s, 4H), 3.96 (t, 4H, J = 6.5 Hz), 3.92 (t, 8H, J = 6.5 Hz), 1.65–1.78 (m, 12H), 1.36–1.58 (m, 12H), 0.95 (t, 6H, J = 7.4 Hz), and 0.92 (t, 12H, J = 7.4 Hz) ppm; ^{13}C NMR (75 MHz, chloroform-d_1) δ 153.8, 153.3, 149.7, 138.1, 131.4, 131.3, 125.4, 117.9, 114.3, 105.8, 92.6, 90.2, 73.1, 71.8, 68.9, 32.3, 31.4, 19.2, 19.2, 13.9, and 13.8 ppm; HRMS (ESI$^+$) calcd for $C_{58}H_{73}O_8N_2$ m/z 925.5361 $[M + H]^+$, found m/z 925.5358; Anal. calcd for $C_{58}H_{72}O_8N_2$ C 75.29, H 7.84, N 3.03, found C 75.60, H 8.17, N 3.07%.

1,4-Bis(4′-pyridylethynyl)-2,5-bis{[3,4,5-tri(hexoxy)phenyl]-methoxy}benzene (2b). A mixture of **5** (627 mg, 0.549 mmol), 4-ethynylpyridine (170 mg, 1.64 mmol), $PdCl_2(PPh_3)_2$ (20 mg, 28 μmol), and CuI (5.3 mg, 28 μmol) in dry THF (5 mL) and dry diisopropylamine (1.5 mL) was stirred for 6 h at rt. The reaction mixture was diluted with ethyl acetate, and the resulting insoluble solid was filtered off. The organic layer was washed with aqueous ammonium chloride solution, dried over anhydrous sodium sulfate, and concentrated. The crude product was purified through recrystallization from ethyl acetate to give a yellow powder (478 mg, 80%). M.p. 82–85 °C; ^{1}H NMR (300 MHz, chloroform-d_1) δ 8.59 (d, 4H, J = 5.9 Hz), 7.34 (d, 4H, J = 5.9 Hz), 7.13 (s, 2H), 6.69 (s, 4H), 5.06 (s, 4H), 3.95 (t, 4H, J = 6.5 Hz), 3.91 (t, 8H, J = 6.5 Hz), 1.66–1.85 (m, 12H), 1.21–1.54 (m, 12H), 0.90 (t, 6H, J = 7.4 Hz), and 0.88 (t, 12H, J = 7.4 Hz) ppm; ^{13}C NMR (75 MHz, chloroform-d_1) δ 153.8, 153.3, 149.7, 138.0, 131.5, 131.3, 125.4, 117.9, 114.3, 105.7, 92.6, 90.2, 73.5, 71.8, 69.2, 31.8, 31.5, 30.3, 29.3, 25.8, 25.7, 22.7, 22.6, 14.1, and 14.0 ppm; HRMS (ESI$^+$) calcd for $C_{70}H_{97}O_8N_2$ m/z 1093.7239 $[M + H]^+$, found m/z 1093.7236; Anal. calcd for $C_{70}H_{96}O_8N_2{\cdot}0.2H_2O$ C 76.63, H 8.86, N 2.55, found C 76.27, H 9.06, N 2.50%.

1,4-Bis(4′-pyridylethynyl)-2,5-bis{[3,4,5-tri(dodecoxy)phenyl]-methoxy}benzene (2c). A mixture of 1,4-diiodo-2,5-bis{[3,4,5-tri(dodecoxy)phenyl]methoxy}benzene[12] (706 mg, 0.429 mmol), 4-ethynylpyridine (111 mg, 1.07 mmol), $PdCl_2(PPh_3)_2$ (15 mg, 21 μmol), and CuI (4.0 mg, 21 μmol) in dry THF (11 mL) and dry diisopropylamine (1.2 mL) was stirred for 6 h at rt. The reaction mixture was diluted with ethyl acetate, and the resulting insoluble solid was filtered off. The organic layer was washed with aqueous ammonium chloride solution, dried over anhydrous sodium sulfate, and concentrated. The crude product was purified through recrystallization from ethyl acetate to give a yellow powder (300 mg, 43%). M.p. 78–81 °C; ^{1}H NMR (300 MHz, chloroform-d_1) δ 8.60 (d, 4H, J = 5.9 Hz), 7.43 (d, 4H, J = 5.9 Hz), 7.13 (s, 2H), 6.68 (s, 4H), 5.06 (s, 4H), 3.95 (t, 4H, J = 6.5 Hz), 3.92 (t, 8H, J = 6.5 Hz), 1.62–1.81 (m, 12H), 1.15–1.56 (m, 108H), and 0.82–0.92 (m, 18H) ppm; ^{13}C NMR (75 MHz, chloroform-d_1) δ 153.8, 153.3, 149.7, 138.0, 131.4, 131.1, 125.3, 117.8, 114.3, 105.7, 92.6, 90.0, 73.4, 71.7, 69.1, 31.9, 30.3, 29.7, 29.6, 29.6 29.4, 29.3, 26.1, 26.1, 22.6, and 14.0 ppm; HRMS (ESI$^+$) calcd for $C_{106}H_{169}O_8N_2$ m/z 1598.2874 $[M + H]^+$, found m/z 1598.2872; Anal. calcd for $C_{106}H_{168}O_8N_2$ C 79.65, H 10.59, N 1.75, found C 79.33, H 10.68, N 1.59%.

1,4-Bis(4′-pyridylethynyl)-2,5-bis{[3,4,5-tri(tetradecoxy)phenyl]-methoxy}benzene (2d). A mixture of **5** (362 mg, 0.210 mmol), 4-ethynylpyridine (65.0 mg, 0.61 mmol), $PdCl_2(PPh_3)_2$ (7.5 mg, 11 μmol), and CuI (2.0 mg, 11 μmol) in dry THF (2.1 mL) and dry diisopropylamine (0.6 mL) was stirred for 6 h at rt. The reaction mixture was diluted with ethyl acetate, and the resulting insoluble solid was filtered off. The organic layer was washed with aqueous ammonium chloride solution, dried over anhydrous sodium sulfate, and concentrated. The crude product was purified through recrystallization from ethyl acetate to give a yellow powder (160 mg, 60%). M.p. 72–76 °C; ^{1}H NMR (300 MHz, chloroform-d_1) δ 8.59 (d, 4H, J = 5.9 Hz), 7.34 (d, 4H, J = 5.9 Hz), 7.13 (s, 2H), 6.69 (s, 4H), 5.06 (s, 4H), 3.95 (t, 4H, J = 6.5 Hz), 3.91 (t, 8H, J = 6.5 Hz), 1.62–1.81 (m, 12H), 1.15–1.56 (m, 132H), and 0.82–0.92 (m, 18H) ppm; ^{13}C NMR (75 MHz, chloroform-d_1) δ 153.8, 153.3, 149.7, 138.0, 131.4, 131.3, 125.6, 117.8, 114.3, 105.7, 92.6, 90.2, 73.4, 71.8, 69.2, 31.9, 30.3, 29.7, 29.7, 29.6, 29.4, 29.4, 26.1, 26.1, 22.7, and 14.1 ppm; HRMS (ESI$^+$) calcd for $C_{118}H_{193}O_8N_2$ m/z 1766.4752 $[M + H]^+$, found m/z 1766.4758; Anal. calcd for $C_{118}H_{192}O_8N_2$ C 80.22, H 10.95, N 1.59, found C 79.91, H 11.09, N 1.47%.

1,4-Bis(4′-pyridylethynyl)-2,5-bis{[3,4,5-tri(octadecoxy)phenyl]-methoxy}benzene (2e). A mixture of **6** (1.04 g, 0.481 mmol), 4-ethynylpyridine (174 mg, 1.69 mmol), $PdCl_2(PPh_3)_2$ (17.1 mg, 24 μmol), and CuI (4.7 mg, 24 μmol) in dry THF (5 mL) and dry diisopropylamine (1.3 mL) was stirred for 6 h at rt. The reaction mixture was diluted with ethyl acetate, and the resulting insoluble solid was filtered off. The organic layer was washed with aqueous ammonium chloride solution, dried over anhydrous sodium sulfate, and concentrated. The crude

product was purified through recrystallization from ethyl acetate to give a yellow powder (480 mg, 48%). M.p. 101–104 °C; ^{1}H NMR (300 MHz, chloroform-d_1) δ 8.60 (d, 4H, J = 5.9 Hz), 7.33 (d, 4H, J = 5.9 Hz), 7.13 (s, 2H), 6.69 (s, 4H), 5.06 (s, 4H), 3.95 (t, 4H, J = 6.5 Hz), 3.91 (t, 8H, J = 6.5 Hz), 1.62–1.81 (m, 12H), 1.15–1.56 (m, 156H), and 0.82–0.92 (m, 18H) ppm; ^{13}C NMR (75 MHz, chloroform-d_1) δ 153.9, 153.3, 149.7, 138.1, 131.4, 131.3, 125.4, 117.9, 114.3, 105.8, 94.4, 92.7, 73.5, 71.9, 69.2, 31.9, 30.4, 29.8, 29.7, 29.7, 29.4, 29.4, 26.1, 26.1, 22.7, and 14.1 ppm; HRMS (ESI$^+$) calcd for $C_{142}H_{241}O_8N_2$ m/z 2102.8508 $[M + H]^+$, found m/z 2102.8529; Anal. calcd for $C_{142}H_{240}O_8N_2$ C 81.08, H 11.50, N 1.33, found C 81.20, H 11.53, N 1.21%.

Acknowledgements

This work was supported by Grant-in-Aids for Scientific Research (B) (No. 24350060) and Challenging Exploratory Research (No. 23655105) from Japan Society for the Promotion of Science (JSPS).

References

1 (*a*) P. Terech and R. G. Weiss, *Chem. Rev.*, 1997, **97**, 3133–3159; (*b*) O. Gronwald and S. Shinkai, *Chem.–Eur. J.*, 2001, **7**, 4328–4334; (*c*) J. H. van Esch and B. L. Feringa, *Angew. Chem., Int. Ed.*, 2000, **39**, 2263–2266; (*d*) D. J. Abdallah and R. G. Weiss, *Adv. Mater.*, 2000, **12**, 1237–1247; (*e*) M. Suzuki and K. Hanabusa, *Chem. Soc. Rev.*, 2009, **38**, 967–975.

2 M. George and R. G. Weiss, *Acc. Chem. Res.*, 2006, **39**, 489–497.

3 (*a*) F. J. M. Hoeben, P. Jonkheijm, E. W. Meijer and A. P. H. J. Schenning, *Chem. Rev.*, 2005, **105**, 1491–1546; (*b*) A. Ajayaghosh and V. K. Praveen, *Acc. Chem. Res.*, 2007, **40**, 644–656.

4 A. P. H. J. Schenning and E. W. Meijer, *Chem. Commun.*, 2005, 3245–3258.

5 (*a*) K. Murata, M. Aoki, T. Nishi, A. Ikeda and S. Shinkai, *J. Chem. Soc., Chem. Commun.*, 1991, 1715–1718; (*b*) S. van der Laan, B. L. Feringa, R. M. Kellogg and J. van Esch, *Langmuir*, 2002, **18**, 7136–7140; (*c*) J. Eastoe, M. Sanchez-Dominguez, P. Wyatt and R. K. Heenan, *Chem. Commun.*, 2004, 2608–2609; (*d*) N. S. S. Kumar, S. Varghese, G. Narayan and S. Das, *Angew. Chem., Int. Ed.*, 2006, **45**, 6317–6321; (*e*) S. Miljanic, L. Frkanec, Z. Meic and M. Zinic, *Eur. J. Org. Chem.*, 2006, 1323–1334; (*f*) M. Moriyama, N. Mizoshita and T. Kato, *Bull. Chem. Soc. Jpn.*, 2006, **79**, 962–964; (*g*) S. Wang, W. Shen, Y. L. Feng and H. Tian, *Chem. Commun.*, 2006, 1497–1499; (*h*) Y. Ji, G. C. Kuang, X. R. Jia, E. Q. Chen, B. B. Wang, W. S. Li, Y. Wei and J. Lei, *Chem. Commun.*, 2007, 4233–4235; (*i*) S. Matsumoto, S. Yamaguchi, A. Wada, T. Matsui, M. Ikeda and I. Hamachi, *Chem. Commun.*, 2008, 1545–1547; (*j*) Y. Sako and Y. Takaguchi, *Org. Biomol. Chem.*, 2008, **6**, 3843–3847; (*k*) Y. Zhou, M. Xu, J. Wu, T. Yi, J. Han, S. Xiao, F. Li and C. Huang, *J. Phys. Org. Chem.*, 2008, **21**, 338–343; (*l*) J. H. Kim, M. Seo, Y. J. Kim and S. Y. Kim, *Langmuir*, 2009, **25**, 1761–1766; (*m*) K. Murata, M. Aoki, T. Suzuki, T. Harada, H. Kawabata, T. Komori, F. Ohseto, K. Ueda and S. Shinkai, *J. Am. Chem. Soc.*, 1994, **116**, 6664–6676; (*n*) A. Shumburo and M. C. Biewer, *Chem. Mater.*, 2002, **14**, 3745–3750.

6 (*a*) K. Hanabusa, T. Miki, Y. Taguchi, T. Koyama and H. Shirai, *J. Chem. Soc., Chem. Commun.*, 1993, 1382–1384; (*b*) X. D. Xu, M. Ayyagari, M. Tata, V. T. John and G. L. Mcpherson, *J. Phys. Chem.*, 1993, **97**, 11350–11353; (*c*) R. Oda, I. Huc, M. Schmutz, S. J. Candau and F. C. MacKintosh, *Nature*, 1999, **399**, 566–569; (*d*) K. S. Partridge, D. K. Smith, G. M. Dykes and P. T. McGrail, *Chem. Commun.*, 2001, 319–320; (*e*) J. R. Moffat and D. K. Smith, *Chem. Commun.*, 2008, 2248–2250.

7 (*a*) M. Ayabe, T. Kishida, N. Fujita, K. Sada and S. Shinkai, *Org. Biomol. Chem.*, 2003, **1**, 2744–2747; (*b*) Y. L. Zhao and J. F. Stoddart, *Langmuir*, 2009, **25**, 8442–8446; (*c*) S. Yagai, T. Nakajima, K. Kishikawa, S. Kohmoto, T. Karatsu and A. Kitamura, *J. Am. Chem. Soc.*, 2005, **127**, 11134–11139.

8 (*a*) M. Tanaka, T. Haino, K. Ideta, K. Kubo, A. Mori and Y. Fukazawa, *Tetrahedron*, 2007, **63**, 652–665; (*b*) T. Haino, M. Tanaka, K. Ideta, K. Kubo, A. Mori and Y. Fukazawa, *Tetrahedron Lett.*, 2004, **45**, 2277–2279.

9 (*a*) T. Haino, M. Tanaka and Y. Fukazawa, *Chem. Commun.*, 2008, 468–470; (*b*) T. Haino and H. Saito, *Synth. Met.*, 2009, **159**, 821–826; (*c*) M. Tanaka, T. Ikeda, J. Mack, N. Kobayashi and T. Haino, *J. Org. Chem.*, 2011, **76**, 5082–5091; (*d*) T. Ikeda, T. Masuda, T. Hirao, J. Yuasa, H. Tsumatori, T. Kawai and T. Haino, *Chem. Commun.*, 2012, **48**, 6025–6027.

10 T. Haino and H. Saito, *Aust. J. Chem.*, 2010, **63**, 640–645.

11 V. Amenta, J. L. Cook, C. A. Hunter, C. M. R. Low and J. G. Vinter, *Org. Biomol. Chem.*, 2011, **9**, 7571–7578.

12 X. Zhang and M. Takeuchi, *Angew. Chem., Int. Ed.*, 2009, **48**, 9646–9651.